

Characterization of a low-cost *Eucalyptus camaldulensis* leaves based activated carbon for pharmaceutical residues removal from aqueous solutions

Iman Gouaich^{a,b}, Benaouda Bestani^{a,*}, Zohra Bouberka^b, Joanna Sreńscek-Nazza^c, Beata Michalkiewicz^c, Mokhtar Benzekri-Benallou^a, Ahmed Boucherdoud^{a,d}, Nouredine Benderdouche^a

^aLaboratoire de Structure Elaboration et Application des Matériaux Moléculaires (S.E.A.M.M), Faculté des sciences et de la technologie, Université de Abdelhamid Ibn Badis, Mostaganem, Algeria, Tel.: +213 552329407; Fax: +213 45206476; emails: bestanib@yahoo.fr (B. Bestani), imangouaich@yahoo.com (I. Gouaich), benzekrimokhtar@yahoo.fr (M. Benzekri-Benallou), bo-ahmed@live.fr (A. Boucherdoud), benderdouchen@yahoo.fr (N. Benderdouche)

^bLaboratoire de physico chimie des matériaux, catalyse et environnement, Université des Sciences et de la Technologie Mohamed Boudiaf USTO, Oran, Algeria, email: bouberkazohra@yahoo.fr (Z. Bouberka)

^cDepartment of Catalytic and Sorbent Materials Engineering, Faculty of Chemical Technology and Engineering, West Pomeranian University of Technology in Szczecin, Piastów Ave. 42, 71-065 Szczecin, Poland, emails: jsrenscek@zut.edu.pl (J. Sreńscek-Nazza), Beata.Michalkiewicz@zut.edu.pl (B. Michalkiewicz)

^dFaculté des sciences et de la technologie, Département de Chimie Université Ahmed Zabana, Relizane, Algeria

Received 21 August 2022; Accepted 30 April 2023

ABSTRACT

Due to their significant disposal problem during oil extraction and biofuel production, *Eucalyptus camaldulensis* leaves as an abundant forestry waste in the Mediterranean region, was investigated in this study as a precursor for the preparation of a low-cost adsorbents for the treatment of water laden with ascorbic acid (AA) as contaminant. A single step involving activation and carbonization in which the raw material was impregnated with chemical agent (KOH 20% and 40%) and then thermally decomposed at 600°C to produce K-Eucal-20 and K-Eucal-40 adsorbents, respectively. Prior to adsorption tests, Fourier-transform infrared analysis, pH_{zpc} determination, scanning electron microscopy, X-ray diffraction, Brunauer–Emmett–Teller surface area, iodine number and methylene blue index were performed for structural and surface characterization. Important parameters affecting AA uptake including equilibrium time, adsorbent dose, solution pH and temperature were also evaluated. Adsorption isotherms were better described by the Langmuir model than those of Freundlich and Temkin. The maximum adsorption capacities achieved for AA were 190.80 and 305.78 mg/g, by K-Eucal-20 and K-Eucal-40, respectively. Kinetics was found to obey the pseudo-second-order model. Thermodynamic analysis confirms the spontaneity and endothermicity of AA adsorption process. This study shows that activated *Eucalyptus camaldulensis* leaves can be successfully used as an alternative to the commercially available adsorbents for the removal of such pollutant from liquid media.

Keywords: Pharmaceutical residues; Activated carbon; Adsorption; Isotherm models

* Corresponding author.

1. Introduction

For decades, the world has been witnessing a rapid increasing of surface and ground water pollution mainly linked to human activity such as industrial discharges (heavy metals, dyestuff and chemicals), phytosanitary products (surfactants, agricultural treatment products) and pharmaceutical products (veterinary products and therapeutic molecules such as antibiotics, anticancer drugs and synthetic hormones). Known to save lives and cure diseases, pharmaceuticals have emerged as a new class of environmental contaminants. Their excessive use worldwide by human and veterinary can contaminate the environment with varying concentrations levels in various ways: their residue may infiltrate surface waters during manufacturing process, since they are excreted in trace quantities into the sewage system once being metabolized by humans, finding then their way to water supply after treatment systems. Also, veterinary pharmaceuticals are excreted in soils and surface waters by pasture animals. In addition, unused drugs are often dumped into public water supplies through sinks, toilets, and landfills contributing then to this type of pollution [1].

Since the 1980s, a number of studies have been carried out on the analysis of drug residues in wastewater showing the presence of traces of several pharmaceutical compounds. Thus, their presence in wastewater has been part of major concerns since they become contributors to environmental degradation [2,3]. Largely used material in the pharmaceutical manufacturer, ascorbic acid (vitamin C) can perform to high values of chemical oxygen demand and biochemical oxygen demand promoting bacteria, and another micro-organism once in rivers and fields, causing thus a serious potential threat to the environment. So, their elimination is a must before dumping them in sewage network [4].

In fact, ascorbic acid may be considered as a pharmaceutical residue in some areas such as senior residences where the intake of pharmaceuticals like painkillers, vitamins, analgesic and antipyretic drugs is largely used. These kinds of drugs are also frequently used in hospitals and clinics, especially by the elderly population, for pain relief and disease fighting. High amounts of ascorbic acid are sometimes used for the prevention of viral infections or the slowing of the progression of cancer, although the health benefits are not obvious. In water, ascorbic acid may mainly be found in the form of metabolites-ascorbic acid-2-sulfate, dehydroascorbate, 2,3-diketogulonic acid, erythrulose, threosone, oxalic acid, which justifies the need to monitor their amounts in wastewater in the areas mentioned.

As for toxicity, although ascorbic acid is essential for good health being an antioxidant, a facilitator of iron-absorption, an intake of amount higher than 2 g may cause nausea and diarrhea. These are the main reasons why we used ascorbic acid as a model pharmaceutical pollutant. In addition, ascorbic acid excretion depends mainly on kidneys and sweat. Gastrointestinal, renal and haematological systems are the main target organs for toxicity. In addition, it has been reported that vitamin C was being extensively used as a coronavirus treatment during the pandemic (COVID-19) with varying medication protocols from patient to patient. It has been reported that patients in intensive-care

receive up to 1,500 mg of intravenous vitamin C (3–4 times a day) representing then 16 times the National Institutes of Health's daily recommended dietary allowance, which is just 75–90 mg.

Overuse of medicines has been increasing over the last decade due mainly to ageing population and the improvement of the health systems in many parts of the world, including developing countries. The increase of drug intake has lately dramatically increased, especially in densely-populated areas. Ascorbic acid is an obvious instance of such a phenomenon because it is widely known as a good antioxidant, playing a vital role for bone and blood-vessel health. However, its acute oral toxicity (LD50) is 3,367 mg/kg in mice; it may be mutagenic for mammalian somatic cells, and for bacteria and yeast. Ascorbic acid may cause adverse reproductive and birth effects based on animal test data. It passes through the placenta and is secreted through maternal milk in humans. An intake of amount higher daily may promote iron overload in patients with thalassemia. Ingestion of large amounts of ascorbic acid may cause gastrointestinal tract irritation, hypermotility, diarrhea, acidification of urine resulting in stone formation in the urinary tract. In some people, vitamin C might cause side effects such as stomach cramps, nausea, heartburn, and headache. The chance of getting these side effects increases with higher doses.

In order to reduce its harmful effect by lowering the concentration, several processes of wastewater treatment containing this emergent pollutant, are in general implemented such as biological processes [5], advanced oxidation processes [6], electrocoagulation [7] and in particular, the technique of adsorption using activated carbons as adsorbents developed from wide range of materials [8–13] has gained much scientific attention in the last decades since it is economical, efficient and highly selective method for the removal of variety of pollutants from wastewater, air, food, beverages and pharmaceuticals.

With a highly developed porosity and an extended surface area, activated carbons are the most commonly used adsorbents in a growing range of health, environmental, safety and industrial applications such as pharmaceuticals removal from wastewater [14,15]. They are mostly prepared from available raw materials and agricultural by-products. By being lignocellulosic materials with relatively high carbon content, *Eucalyptus* leaves, a raw material abundantly available locally, presenting no value and often presenting expensive disposal problems [16] after essential oil extraction were chosen in this study as an alternative for activated carbon production for ascorbic acid removed from simulated wastewater.

The massive use of ascorbic acid during the last 3–4 y (COVID-19) has resulted to the release of large quantities, thus increasing water pollution in all its form. The aim of this research work is to propose a way to clean up this water loaded with this type of pharmaceutical species by using a cheaper adsorbent obtained from locally available lignocellulosic waste. The waste chosen in our case is the *Eucalyptus* leaves obtained from essential oil extraction plants. Using chemical and physical methods, leaves were valorized by converting them into activated carbon for the above-mentioned pollutant removal from aqueous solutions and to

solve the storage problem caused by the huge amount of waste left when separated from its essential oil.

2. Materials and methods

2.1. Solutions preparation

Stock solution of the relevant substance of ascorbic acid (from Saidal – Algeria, 99% purity) of known concentrations were prepared according to the standard procedure by dissolving 500 mg of the substance in 1 L flask using distilled water. Working solutions of desire concentrations were prepared by successive dilutions using distilled water. Potassium hydroxide (purchased from Sigma-Aldrich, Germany). Analytical reagent-grade chemicals were used for solutions preparation. Table 1 shows some important properties of ascorbic acid.

2.2. Adsorbent preparation

The biomass used in the trials – *Eucalyptus camaldulensis* leaves a widespread lignocellulosic plant found in the Mediterranean region – was collected from (Mostaganem region-west of Algeria) washed with tap water to remove dust, then dried in sunlight and oven heated at 100°C overnight, ground using a jar mill (Vierzen grinder) to increase the reactivity and sieved to pass through a 0.14 mm sieve (obtained sample was called NT-Eucal). For adsorptive properties enhancement, 50 g of *Eucalyptus camaldulensis* leaves were simultaneously pyrolyzed in a tubular furnace (Nabertherm LE14 C290/11) at 400°C then impregnated separately in known potassium hydroxide solution (20% and 40%) in order to activate the material pores. The mixtures were agitated for 24 h at ambient, filtered, dried and then pyrolyzed again at 600°C for 1 h. The obtained K-Eucal-20 and K-Eucal-40 samples described by Fig. 1, were washed with HCl solution (0.1 N) then with hot distilled water till constant pH, filtered, oven-dried overnight at 105°C and kept in desiccators before adsorption tests.

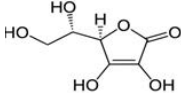
2.3. Adsorbent characterization

2.3.1. Iodine and methylene blue adsorption for surface area estimation

Known as relative indicators of adsorbents available surface area, iodine number and methylene blue index were evaluated in this study. Having a surface occupied by one molecule equal 20.96 Å², iodine number defined in mg of I₂ adsorbed by 1 g of adsorbent is mainly adsorbed in micropores giving then a good approximation of the samples microporosity according to ASTM D-4607 standard method [17] and described in previous work [18]. However, by having a surface occupied by one larger molecule, methylene blue as a typical dye is mainly adsorbed in larger pores for better mesoporosity approximation according to Chemviron Carbon TM-11 standard method (Zoning Industriel C, B-7181 Feluy, Belgium). The mesoporous available surface is then calculated using the following equation:

$$S_{BM} = \frac{b \times N_A \times A_{BM}}{M_{BM}} \quad (1)$$

Table 1
Chemical structure and characteristics of adsorbed ascorbic acid

	Ascorbic acid
Structure	
IUPAC name	(2R)-2-[(1S)-1,2-dihydroxyethyl]-3,4-dihydroxy-2H-furan-5-one
Molecular formula	C ₆ H ₈ O ₆
Molecular weight (g/mol)	176.124
Density (g/cm ³)	1.65
Solubility (g/L at 20°C)	300
CAS number	50-81-7

where S_{MB} is the surface area (m²/g), b is maximum adsorption capacity (mg/g) based on a monolayer coverage (determined previously from the Langmuir model), N_A is Avogadro's number (6.023×10^{23} mol⁻¹), A_{MB} is the surface occupied by one molecule of methylene blue (taken as 119 Å²), and M_{MB} is the molecular weight of methylene blue (319.86 g/mol).

2.3.2. Brunauer–Emmett–Teller analysis for surface area estimation

Nitrogen adsorption–desorption measurements at 77 K were performed using Quadrasorb evo™ Gas Sorption analyzer (Anton Paar) to obtain a specific surface area, total pore volume and pore-size distribution. To calculate the specific surface area (S_{BET}) Brunauer–Emmett–Teller equation was applied. Total pore volume was estimated based on the N₂ volume adsorbed at the P/P_0 1. Pore size distribution was calculated by Barrett–Joyner–Halenda method.

2.3.3. pH of zero-point charge (pH_{zpc})

Commonly used to indicate the adsorbent net surface charge in solution is the point of zero charge (pH_{zpc}), pH for which the net surface charge is equal to zero. It is also used to predict solid–liquid affinity. Obtained from the intersection point of ($pH_{final} - pH_{initial}$) vs. $pH_{initial}$ plot, the adsorbent surface is considered to be positively charged at $pH < pH_{zpc}$ and negatively charged at $pH > pH_{zpc}$. To do this, experiments were carried out as follows: initially; 50 mL of 0.01 M NaCl solutions were put into several closed Erlenmeyer flasks. The pH within each flask was adjusted to a value ranging from 2 to 12 by adding HCl (0.1 M) or NaOH (0.1 M) solutions, measured once stabilized and noted as $pH_{initial}$. Then, 0.15 g of activated carbon sample was added into each flask. After 48 h of magnetically agitation pH news were measured and noted as pH_{final} . The pH_{zpc} is the value at which both pHs are equal ($pH_{initial} = pH_{final}$) [19].

2.3.4. IRFT-surface functional groups determination

Infrared analysis was used for principal functional groups identification present at the surface of the adsorbent.

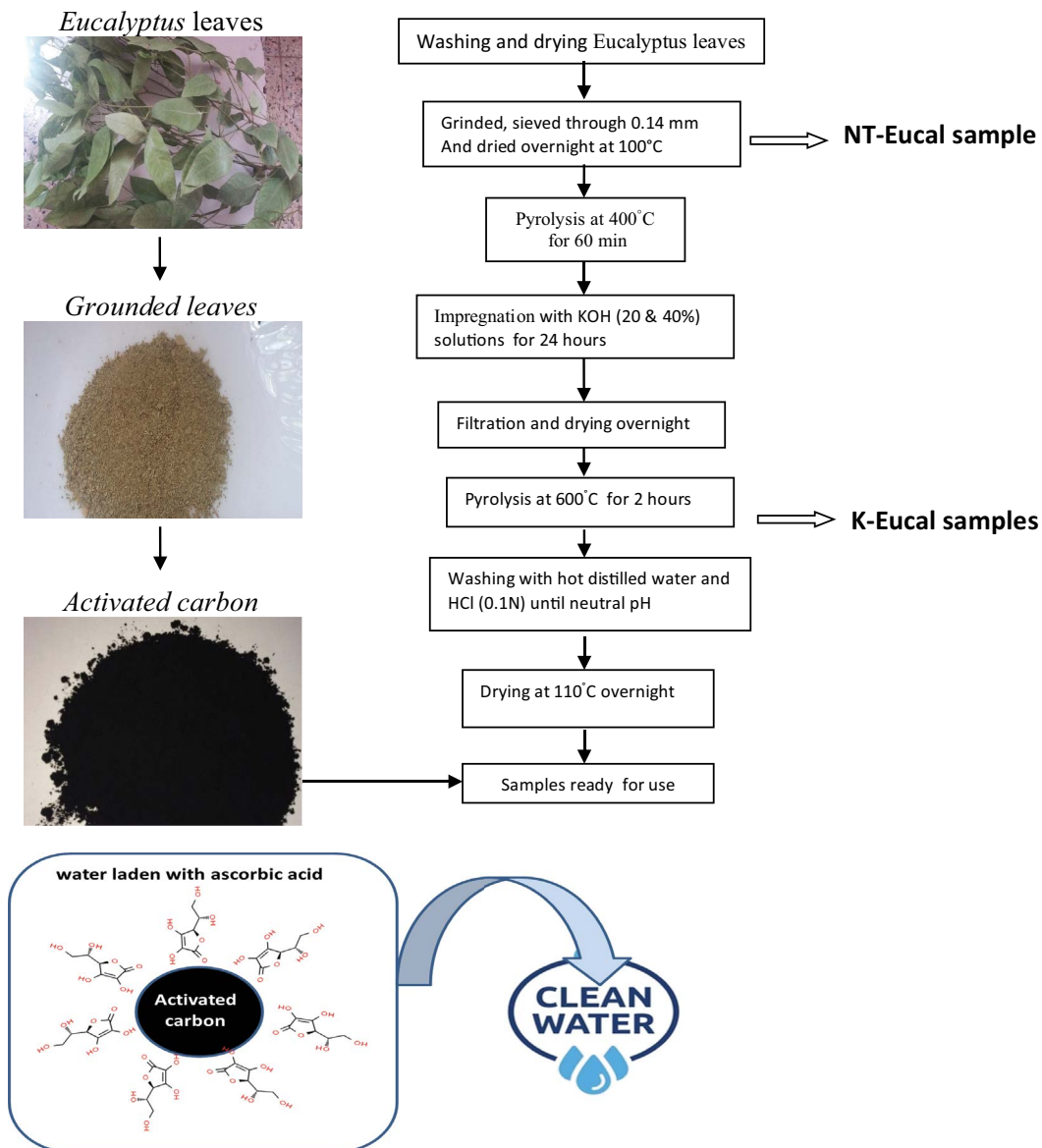


Fig. 1. Steps-process carried out on activated process on *Eucalyptus camaldulensis* leaves (Cases: NT-Eucal, K-Eucal-20 and K-Eucal-40 adsorbents preparation).

The IR spectra were determined using sampling in KBr on an IRPrestige-21, SHIMADZU spectrometer. In addition, scanning electron microscopy observations (SEM) analysis was also performed for samples characterization using SU8020 Ultra-High Resolution Field Emission Scanning Electron Microscope; Hitachi Ltd., Japan, 2012.

2.3.5. Burn-off

Defined as the ratio of % weight decrease of the material during the preparation to the original weight of the raw material, burn-off is often used to evaluate the degree of activation process and it can be determined from the following equation.

$$\text{Burn-off (\%)} = \frac{M_i - M_f}{M_i} \times 100 \quad (2)$$

where M_i is the initial mass (g) of the raw material and M_f is the product final mass (g).

2.4. Batch adsorption studies

Adsorption studies on batch mode were performed by mixing an amount of adsorbent (initially chosen on the basis that it was the dosage giving a high removal rate) in stoppered conical flasks with 25 mL of ascorbic acid solutions of known concentration. The resulting suspension was then agitated magnetically at ambient. After the adsorption process had occurred, the solutions were centrifuged at 5,000 rpm for 15 min and the supernatants were analyzed by spectrophotometry for the determination of remaining concentrations in the solution. Experiments were repeated in triplicate and the average values were reported for further

calculations. Also experiments were carried out at different parameters affecting adsorption rate, such as pH range 2–8, initial dye concentration range 25–125 mg/L, contact time range 0–240 min, adsorbent dose range 2–12 g/L and temperatures equal to 293, 298 and 303 K.

Analyses for supernatant concentrations were performed using a UV-Vis spectrophotometer (SHIMADZU-Europe UV mini – 1240) to determine the extent of ascorbic acid removal from which the amount retained by the solid phase (q_e) was determined according to the mass balance represented by the following relationship:

$$q_e = \frac{(C_0 - C_e)V}{1000m} \quad (3)$$

3. Results and discussion

3.1. Samples characterization

The samples were characterized prior to adsorption tests using different chemical and physico-chemical methods such as available surface area via iodine number, and methylene blue index, pH_{zpc} , Fourier-transform infrared analyses, scanning electron microscopy, Brunauer–Emmett–Teller (BET) and X-ray diffraction.

3.1.1. Mesoporous and microporous available areas

As reported in previous works [17], classical standard methods were used for global porosities determination of both samples such as iodine number related to the microporosity, expressed in mg of iodine per g of adsorbent since it has been reported in the literature that 1 mg of iodine adsorbed is approximately equal 1 m^2/g [20]. As expected, the iodine numbers of treated *Eucalyptus* leaves (K-Eucal-20 and K-Eucal-40) increase compared to their untreated states. This is due to the removal of VOCs and impurities from samples as a result of their simultaneous treatments (chemical and thermal) that have undergone, creating then more porous spaces. For larger pores related to the mesoporosity evaluation, methylene blue index was used for this purpose. Values of iodine number, methylene blue index and its available area (S_{MB}) are

summarized in Table 2. Samples treatment conditions of 24 h impregnation (20 and 40 wt.%) and then heating at 600°C for 1 h, were effective in developing microporosity for K-Eucal-40 (iodine number = 673 mg/g) and mesoporosity for K-Eucal-20 (MB index = 62.72 mg/g).

3.1.2. pH_{zpc} determination

The point where the adsorbent do not induce the release of either H^+ or OH^- ions into the solution (net surface charge is equal to zero) is called the pH_{zpc} . Values of the latter are indicated by the intersection point of ($\Delta\text{pH} = \text{pH}_{\text{initial}} - \text{pH}_{\text{final}}$) vs. ($\text{pH}_{\text{initial}}$) plots shown in Fig. 2. As seen from Fig. 2, there is a distinct common point of intersection at $\Delta\text{pH} = 0$ line at $\text{pH}_{\text{initial}} = 8.20$ and 8.40, corresponding to the pH_{zpc} values of K-Eucal-20 and K-Eucal-40 adsorbents, respectively which is in accordance of the activating agent used in this study. The pH_{zpc} is also related to functional groups (acid or basic) on the adsorbent surface usually determined by infrared analysis.

3.1.3. Burn-off and moisture content

3.1.3.1. Burn-off

The degree of burn off is often used to evaluate the extent of activation [21,22]. Activated carbons pores enlargement

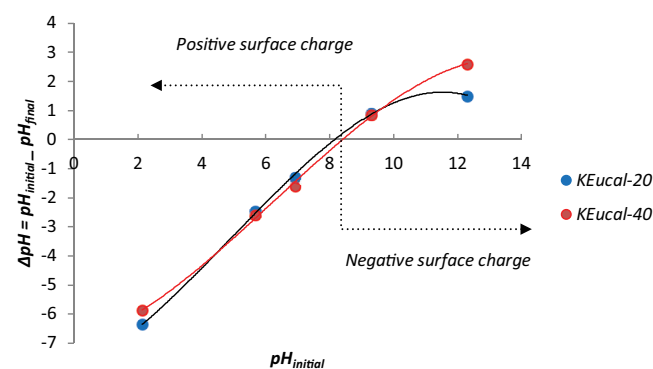


Fig. 2. pH change of K-Eucal-40 and K-Eucal-20 adsorbents as a function of $\text{pH}_{\text{initial}}$.

Table 2
Characteristics of prepared samples surfaces

Adsorbents	NT-Eucal*	K-Eucal-20	K-Eucal-40
Iodine number (mg/g)	446	475.87	673.00
Methylene blue index (mg/g)	//	62.70	28.25
S_{MB} available area (m^2/g)	//	140.51	63.30
S_{BET} (m^2/g)	//	92.00	200.00
Total pore volume (cm^3/g)	//	0.138	0.075
Pore diameter (Å)	//	94.44	85.98
Efficiency (%)	//	79.00	62.12
Burn-off (%)	//	21.00	37.88
Moisture (wt.%)	//	1.03	1.46
pH_{zpc}	6.37	8.40	8.45

*NT-Eucal: non-treated *Eucalyptus* leaves.

generally occurs at high burn-off. But due to the ablation of the external surface of the carbon particles, precursors very rarely go beyond 50% because production is dominated by the compromise between porosity development and yield of the process. The obtained burn-off values of 21.00% and 37.88% for K-Eucal-20 and K-Eucal-40 samples are well below the recommended maximum value producing then an increase in micropore and mesopores spaces in agreement with the iodine number and methylene blue available area values represented in Table 2.

3.1.3.2. Moisture content

Plays an important role in adsorption capacity determination of activated carbons. It involves heating the adsorbents to a temperature slightly above the boiling point of water (377–383 K) and holding it at that temperature until no further weight loss is observed.

The average moisture content of the K-Eucal-20 and K-Eucal-40 samples, respectively 1.03 and 1.46. Lowering the moisture content, results better in adsorption capacity of ascorbic acid, because water vapors compete in adsorption process and fill the adsorption sites within the pores, thus reducing the adsorbents efficiency [23,24].

3.1.4. Functional groups identification by Fourier-transform infrared spectroscopy

The principal functional groups present at the surface of *Eucalyptus* leaves biosorbent and *Eucalyptus* leaves-based activated carbons, were identified using the Infrared analysis in the 4,000–400 cm^{-1} range. The infrared transmission spectra of the powdered raw *Eucalyptus* (NTEuca) and *Eucalyptus*-based activated carbon materials (K-Eucal-20 and K-Eucal-40) are shown in Fig. 3. They exhibit a number of bands or peaks, which correspond to hydroxyl groups (ν -OH) of carboxylic acids, phenols or alcohols, and adsorbed water (strong band at 3,438.57 cm^{-1}). Furthermore, the absorption peak at 2,937.6 cm^{-1} could be attributed to the valence vibration of C–H (stretching). The adsorption peak at 1,644.91 cm^{-1} confirms the presence of the carboxyl group

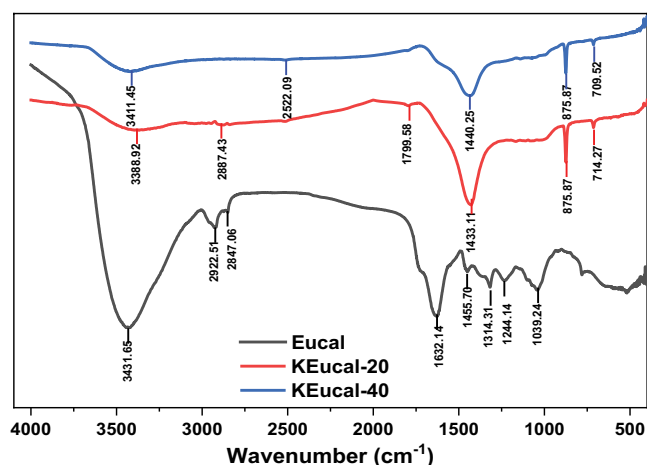


Fig. 3. Fourier-transform infrared spectrum of K-Eucal-40 and K-Eucal-20 sample insert: raw *Eucalyptus* leaves.

C=O and a weak peak of carbonyl group at 1,321.49 cm^{-1} may be related to the COO^- ion. A band observed at 1,044.14 cm^{-1} may be attributed to an elongation one in the C–O group of acids, alcohols, phenols, ethers or ester groups. Peaks observed at 513.4 cm^{-1} suggest the presence of CH vibrations attributed to cellulose. The IR spectra of K-Eucal-40 and K-Eucal-20 show peaks at 3,324.33 and 3,388.92 cm^{-1} , respectively, that can be attributed to hydroxyl groups vibrations. The spectrum between 2,949 and 2,522 cm^{-1} can be attributed to elongation vibrations of C–H/OH and C–H group of CHO. Peaks ranging between 1,713 and 1,627 cm^{-1} can be attributed to the symmetric C=C and C=O stretching of pyrone, aldehyde or carboxylic groups. Signals 1,428.98 and 1,433.11 cm^{-1} for both samples correspond to the C–O bonding of phenols, carboxylic acid or ester. Elongation bands in the C–O of acids, alcohols, phenols, ethers or ester groups are detected at 1,143.95 and 1,174.64 cm^{-1} . Peaks at 670 and 802.8 cm^{-1} suggest the existence of halogen groups.

3.1.4. Samples surface morphology

The microstructure of *Eucalyptus* leaves-based activated carbons was examined by SEM. Fig. 4 gives an overview on the surface *Eucalyptus* leaves-based activated carbons (K-Eucal-20 and K-Eucal-40 samples). A relatively heterogeneous non-porous surface was observed for the raw material in which the particles are mainly arranged in layers, they possess a cotton-like appearance with almost no voids or cavities as expected, since it did not undergo any treatment. Furthermore, K-Eucal-40 sample presents a relatively heterogeneous surface, as well as the presence of cavities, as a result of the activating agent reaction on its surface compared to K-Eucal-20, where almost a clear surface is shown.

3.1.5. Identification of crystalline phases

X-ray diffraction analysis is performed on *Eucalyptus* leaves-based activated carbons powder with a diffractometer (D8 Advance Bruker) in the range of $2\theta: 5^\circ$ to 100° .

The diffractograms (Fig. 5) show that the main structure of both K-Eucal-20 and K-Eucal-40 activated carbons is crystalline. Comparison of the obtained diffractograms with the referenced ones stored in powder diffraction file (pdf) confirms the presence of calcite (CaCO_3 ; peak at 29°) (pdf-03-0596) in both samples. This can be explained by the presence of an amount of calcite in the *Eucalyptus* powder which did not disappear because the low pyrolysis temperature ($<900^\circ\text{C}$). A small peak at 43° in the figure is attributed to the dehydrated hemicellulose. Its appearance shows that the activation process has been correctly performed. The peaks at $\theta = 23.5^\circ$ in the two graphs are attributed to the presence of carbon and graphite. In the case of K-Eucal-40 sample, the characteristic peaks persist but some low intensity peaks have disappeared, which can be explained by the high percentage of KOH (40%).

3.1.6. Surface area determination

Nitrogen adsorption/desorption isotherms at 77 K as a function of relative pressure (P/P_0) of both K-Eucal-20 and K-Eucal-40 samples were performed using the BET

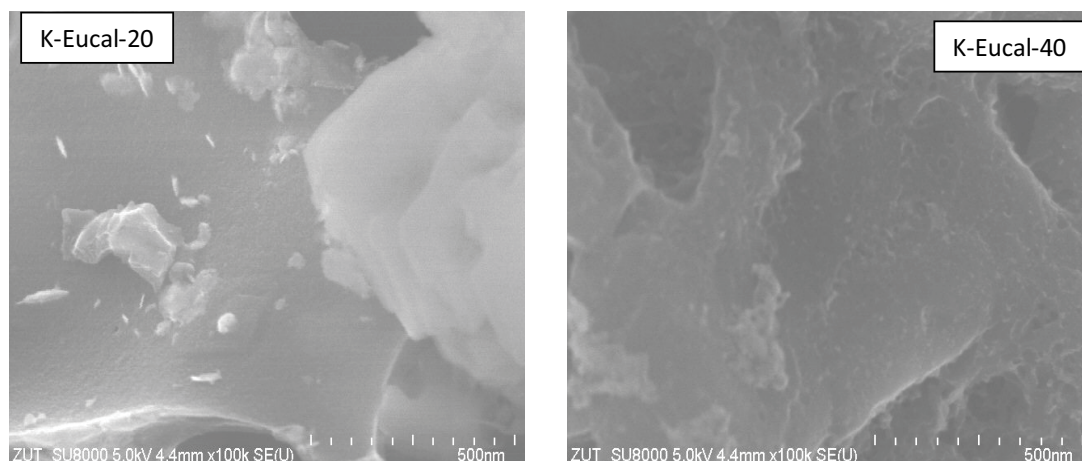


Fig. 4. Scanning electron microscopy images K-Eucal-20 and K-Eucal-40 samples.

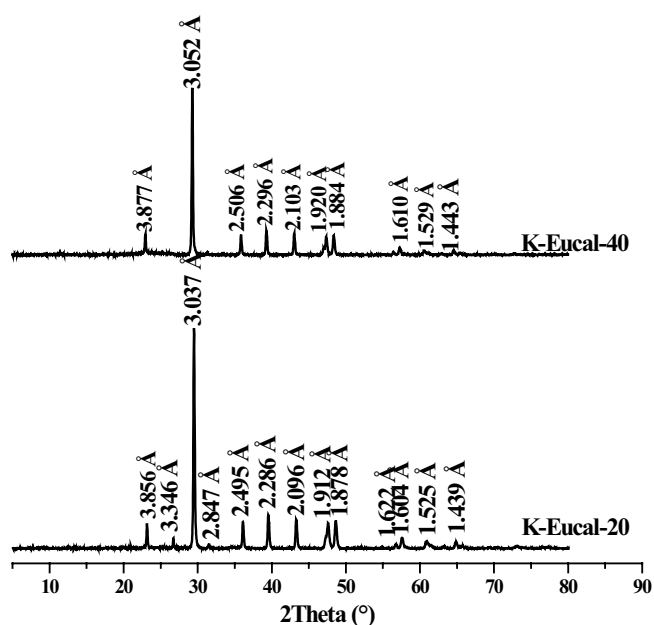


Fig. 5. X-ray diffraction patterns of K-Eucal-20 and K-Eucal-40 samples.

method for their pore structure characterization are shown in Fig. 6. They exhibit type II isotherm, indicating an indefinite multi-layer formation after completion of the monolayer (lower relative P/P_0 values). This type of isotherm is found in adsorbents with a wide range of pore sizes such as macroporous materials. H_3 type hysteresis loop associated to capillary condensation defined by IUPAC [25] is also observed. This is the most common isotherm obtained when using the BET method. A gradual increase of N_2 adsorption reflecting monolayer to multilayer adsorption process is observed at higher P/P_0 values. Slight capillary condensation of N_2 occurs in larger pores. A broader hysteresis loop covering the range of P/P_0 from 0.10 to 0.99 for both samples. The lower values of surface specific area obtained and shown in Table 2 are mainly due to the limited temperature used during the activation for good yield.

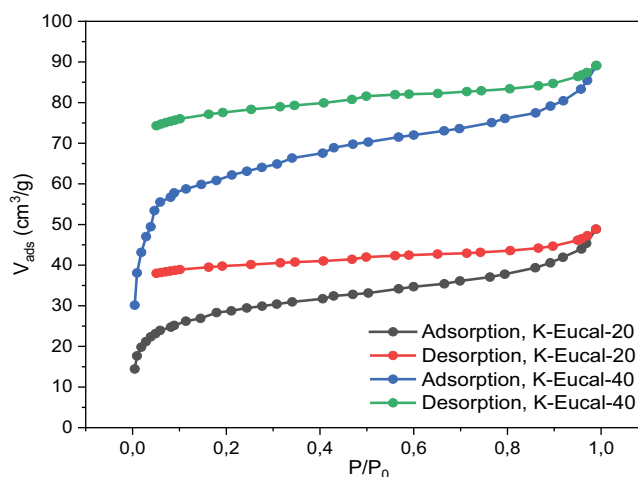


Fig. 6. Adsorption–desorption isotherms of N_2 onto K-Eucal-20 and K-Eucal-40 adsorbents.

To limit high adsorbent weight loss at high temperatures, a value of 600°C was selected as the activation temperature.

3.2. Modeling of adsorption kinetics

Both diffusion and adsorption-controlled models are usually used to evaluate the equilibrium time and to describe the kinetic mechanism of adsorption process. In order to do that, well known models such as Lagergren pseudo-first-order, pseudo-second-order and intraparticle diffusion in their linear forms were used in this study to the experimental data of ascorbic acid uptake onto *Eucalyptus camaldulensis* leaves-based activated carbons.

3.2.1. Lagergren's equation

Also known as Lagergren pseudo-first-order model is based on the assumption that the rate of change of solute uptake with time is directly proportional to difference in saturation concentration and the amount of solid uptake with time, which is generally applicable over the initial

stage of an adsorption process and is given by the following equation.

$$\ln(q_e - q_t) = \ln q_e - k_1 t \tag{4}$$

where q_e and q_t (mg/g) are the amount of pollutant adsorbed at equilibrium and at time t (min), respectively, k_1 (min^{-1}) is the pseudo-first-order adsorption rate constant, t (min) is the contact time. Values of q_e and k_1 determined from the intercept and slope of $\log(q_e - q_t)$ vs. t plots are summarized in Table 3. Adsorption of ascorbic acid data do not obey the pseudo-first-order model in its linear form since R^2 values are lower due to the scattered data (Fig. 7a) and also there is disagreement between the experimental equilibrium adsorption capacities ($q_{e,\text{experimental}}$) and the calculated ones ($q_{e,\text{calculated}}$) (Table 3). Hence, adsorption might not be diffusion-controlled phenomena.

3.2.2. Pseudo-second-order equation

One of the most popular model used to describe adsorption kinetics developed by Ho and McKay [26,27] is given by Eq. (5):

$$\frac{t}{q_t} = \frac{1}{k_2 q_e^2} + \frac{1}{q_e} t \tag{5}$$

where k_2 (g/mg·min) is the rate constant of the second-order equation. Parameters q_e and k_2 are determined from the intercept and slope t/q_t vs. t plots.

As shown in Fig. 7a and b, and in contrast to the pseudo-first-order, the pseudo-second-order model is very representative for ascorbic acid adsorption data in its linear form since the calculated ($q_{e,\text{calculated}}$) values appear to show reasonable agreement with the experimental ($q_{e,\text{experimental}}$) values. In addition, R^2 values are higher. From the above analytical data, it is clear that the pseudo-second-order model provides better correlation of ascorbic acid adsorption onto both samples, suggesting that the rate-limiting step of adsorption process might be the chemisorption,

involving valence forces through sharing or exchange of electrons between the considered adsorbents and the pollutant. Same finding were reported in the literature using different adsorbents [14].

3.2.3. Intraparticle diffusion model

For adsorption kinetics adsorption analysis, a widely used model namely the intraparticle diffusion model proposed by Weber–Morris [28] given by Eq. (6) is used in this

Table 3
Kinetic parameters for ascorbic acid uptake onto K-Eucal-20 and K-Eucal-40

	K-Eucal-20		K-Eucal-40	
C_{Initial} (mg/g)	100	200	100	200
Pseudo-first-order				
$q_{e(\text{exp})}$ (mg/g)	22.24	43.69	23.90	49.87
$q_{e(\text{calc})}$ (mg/g)	1.31	0.908	0.691	0.493
k_1 ($\times 10^2/\text{min}$)	0.0056	0.0136	0.0047	0.015
R^2	0.9429	0.073	0.018	0.17
Pseudo-second-order				
$q_{e(\text{calc})}$ (mg/g)	22.35	45.27	24.34	51.23
k_2 (g/mg·min)	0.115	0.073	0.021	0.016
h (mg/g·min) 10^{-3}	57.04	74.30	78.23	100.00
R^2	1.00	0.988	0.991	0.993
Intraparticle diffusion				
$k_{\text{int-1}}$ (mg/g·min $^{0.5}$)	0.6003	0.0859	0.4383	0.9626
$k_{\text{int-2}}$ (mg/g·min $^{0.5}$)	0.0874	0.1761	0.0889	0.1068
C_1 (mg/g)	19.541	41.750	22.880	45.102
C_2 (mg/g)	21.552	42.529	23.261	49.174
R_1^2	0.999	0.964	0.960	0.992
R_2^2	0.976	0.998	0.747	0.957

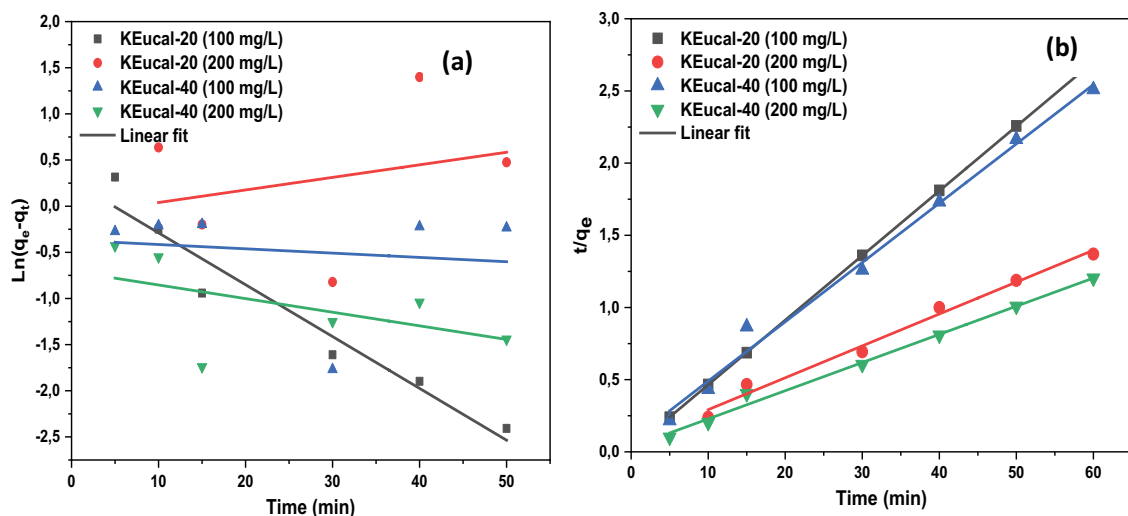


Fig. 7. (a) Pseudo-first-order and (b) pseudo-second-order adsorption kinetics of ascorbic acid onto K-Eucal-20 and K-Eucal-40 samples.

study to interpret experimental kinetics data of ascorbic acid onto both adsorbents.

$$q_t = k_{int}t^{0.5} + C \tag{6}$$

where k_{int} (mg/g·min^{1/2}) is the intraparticle diffusion rate constant, and C (mg/g) is a constant related to the thickness of the boundary layer. C and k_{int} are the intercept and the slope of q_t vs. $t^{1/2}$ plots, respectively. C values determine the boundary layer effect (higher values, the greater the effect). As shown in Fig. 8, two related straight lines were obtained meaning that the adsorption process of ascorbic acid onto K-Eucal-20 and K-Eucal-40 samples is not controlled by intraparticle diffusion only. The first straight line depicting larger pores diffusion in which the external resistance to mass transfer surrounding the particles (boundary layer diffusion) is significant only at the early stage of adsorption process. In the first sharp portion, a rapid adsorption onto adsorbents active sites in which most of the pollutant was adsorbed outward. The second line represents smaller pores diffusion which is the gradual adsorption step with controlling intraparticle diffusion of ascorbic acid from the surface to the internal pores of the adsorbent [29]. The thickness of the boundary layer given by constants C are all positive implying that the intraparticle diffusion is not alone the rate limiting step as seen in Fig. 8.

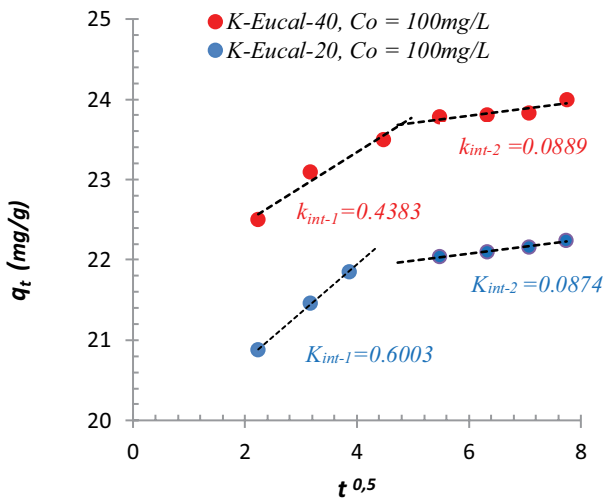


Fig. 8. Intraparticle diffusion for ascorbic acid, onto both samples.

3.3. Modeling of adsorption isotherms

In order to depict the equilibrium adsorption isotherm of ascorbic acid onto K-Eucal-20 and onto K-Eucal-40 samples, both solid and liquid phase concentrations plots were used. Most commonly two-parameter adsorption isotherms equations have been also tested in the present work to fit the experimental data, namely Freundlich isotherm model [30] usually used to describe adsorption tests taking place on heterogeneous adsorbent surface given by Eq. (7), Langmuir model [31] which assumes that the adsorption takes place at specific homogeneous sites within the adsorbent with no further adsorption taking place at a site once filled given by Eq. (8) and Temkin model [32] represented by Eq. (9) which assumes that the energy of adsorption is a linear function of the surface coverage due to adsorbent–adsorbate interactions. Table 4 summarizes linear and non-linear forms of the above-mentioned isotherms models fitted to experimental data to describe the adsorption process of ascorbic acid at the solid–liquid interface.

where q_e is amount of solute adsorbed per unit weight of adsorbent (mg/g), C_e is the solute concentration remaining in solution at equilibrium (mg/L), b (mg/g) is the maximum adsorption capacity corresponding to complete monolayer coverage and K_L is a constant related to the energy or net enthalpy. K_F and n are the Freundlich constants related to adsorption capacity and adsorption intensity. For Temkin isotherm, $B = (RT)/b_T$. T the absolute temperature (K) and R is the universal gas constant (8.314 J/mol·K). The constant b_T is related to the heat of sorption (J/mol) and K_T is the equilibrium Temkin constant corresponding to the maximum binding energy.

The adsorption isotherms of ascorbic acid at working conditions (contact time = 30 min, carbon dosage 4 g/L and pH = 2.5) determined are shown in Fig. 9. The non-linear forms of these isotherms have been used in order to describe in a satisfactory way the uptake of ascorbic acid onto K-Eucal-20 and K-Eucal-40 samples.

From the same figure, we can see that the adsorption rate increases rapidly at low concentrations in solution then attenuates to reach saturation at higher concentrations corresponding to maximum adsorption capacities.

The obtained isotherms models parameters from different plots (Fig. 9) are given in Table 5 from which we can depict the maximum adsorption capacities obtained from Langmuir model onto K-Eucal-40 and K-Eucal-20, respectively 305.78 and 190.80 mg/g. Compared to other adsorbents reported in the literature [14,33–35] and summarized

Table 4
Linear and non-linear forms of Langmuir, Freundlich and Temkin isotherms

Isotherm	Non-linear form	Linear form	Parameters
Freundlich	$q_e = K_F C_e^{1/n}$	$\ln(q_e) = \ln K_F + \left(\frac{1}{n}\right) \ln C_e$	K_F and n from $\ln(q_e)$ vs. $\ln(C_e)$ plots
Langmuir	$q_e = \frac{b K_L C_e}{1 + K_L C_e}$	$\frac{C_e}{q_e} = \left(\frac{C_e}{b}\right) + \left(\frac{1}{b \times K_L}\right)$	K_L and b from (C_e/q_e) vs. (C_e) plots
Temkin	$q_e = B \ln(K_T C_e)$	$q_e = B \ln K_T + B \ln C_e$	K_T and B from q_e vs. $\ln C_e$ plots

in Table 6, implying that the surface modified *Eucalyptus camaldulensis* leaves can be efficiently be used in removing ascorbic acid as a pollutant from wastewater.

In addition, R_L ($R_L = 1/(1 + b \times C_0)$) values ranging between 0 and 1, indicate that ascorbic acid adsorption onto both adsorbents is a favorable process in agreement with the adsorption intensity factor $n > 1$ derived from Freundlich model which states that the magnitude of n depicts the adsorption process favorability, with $2 < n < 10$ (very favorable), $1 < n < 2$ (moderately difficult) and $n < 1$ (poor adsorption potential). The obtained n values are >1 meaning that

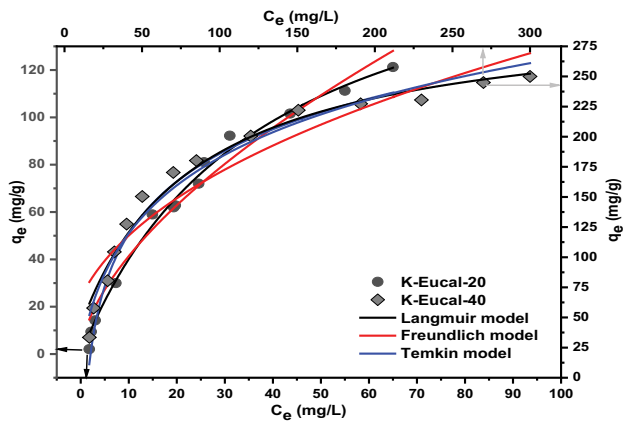


Fig. 9. Adsorption isotherms of ascorbic acid onto K-Eucal-20.

Table 5
Langmuir, Freundlich and Temkin parameters for ascorbic acid removal

		K-Eucal-20	K-Eucal-40
Langmuir	R^2	0.991	0.973
	b (mg/g)	190.80	305.78
	K_L (L/mg)	0.027	0.016
	R_L	3.494×10^{-5}	2.181×10^{-5}
Freundlich	R^2	0.969	0.901
	n	1.657	2.399
	K_F (mg/g)	10.308	24.994
Temkin	R^2	0.960	0.974
	K_T (L/mg)	0.491	0.129
	B	31.895	71.345

Table 6
Maximum adsorption capacities of various adsorbents for ascorbic acid

Adsorbents	q_{max} (mg/g)	References
Activated carbon	520.80	[14]
Fe ₃ O ₄ magnetic nanoparticles	6.90	[33]
PAN:SiO ₂ composite	45.66	[34]
Entrapped activated carbon in alginate	21.59	[35]
Treated <i>Eucalyptus camaldulensis</i> leaves with KOH 20%	190.80	[This study]
Treated <i>Eucalyptus camaldulensis</i> leaves with KOH 40%	305.78	[This study]

the biosorption processes are all favorable and then adsorption process is moderately difficult ($n = 1.657$ to 2.399).

Based on R^2 values, Langmuir model is more representative. Data of all three models studied can be classified in the following order (from best fitting to least one): Langmuir model $>$ Temkin model $>$ Freundlich model. Temkin model was not well represented for ascorbic acid onto K-Eucal-40 with positive B parameters related to the heat of sorption indicating the existence of weak sorbent–sorbate interaction.

By being an anion, negatively charged, ascorbic acid functions are considered to an electron donor or reducing agent. The mechanism of ascorbic acid onto K-Eucal-20 and K-Eucal-40 samples can be explained that in the alkaline media ($pH > 8.5$), lower values of the removal efficiency was observed mainly due to the repulsion between both negatively charged adsorbate and adsorbent surface as shown in pH_{zpc} study (Fig. 2) as OH^- covered the adsorbents surfaces. In the acidic media, the adsorbents surface is positively charged increasing then the electrostatic force of attraction between ascorbic acid and adsorbents surface resulting in an increase of the removal efficiency.

3.4. Thermodynamic study

Thermodynamic functions such as changes in the standard free energy (ΔG°), the enthalpy (ΔH°) and entropy (ΔS°) were evaluated graphically as functions of temperature in order to determine the spontaneity, nature and the adsorbent applicability of ascorbic acid adsorption onto both prepared adsorbents. These functions were calculated from the adsorption distribution coefficient (K_d) using the following equations [36]:

$$K_d = \frac{C_a}{C_e} \quad (10)$$

$$\ln K_d = \frac{\Delta S^\circ}{R} - \frac{\Delta H^\circ}{T} \quad (11)$$

$$\Delta G^\circ = -RT \ln K_d = T\Delta S^\circ - \Delta H^\circ \quad (12)$$

$$\ln S^* = \ln(1 - \theta) - \frac{E_a}{RT} \quad (13)$$

Fig. 10a shows plots of $\ln K_d$ vs. T^{-1} from which ΔS° and ΔH° are obtained using the intercept and the slope, respectively. Thermodynamic functions values are summarized in Table 7. Negative values of ΔG° indicate that nature of

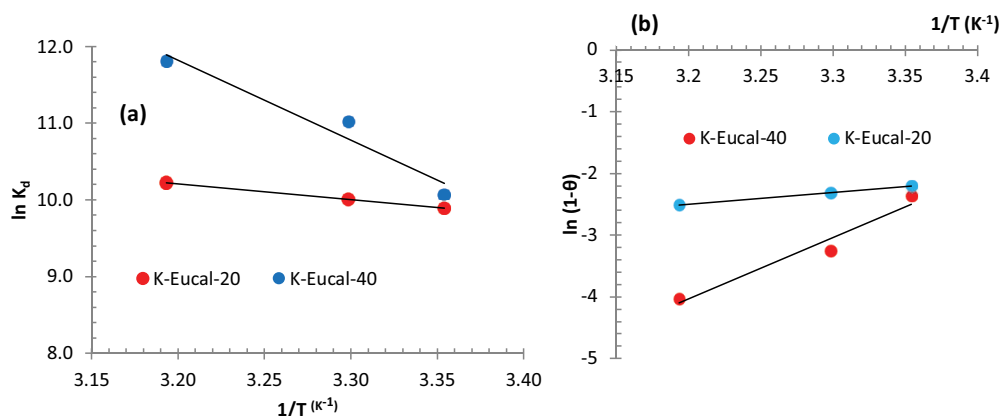


Fig. 10. (a) Van't Hoff plots and (b) modified Arrhenius plots for ascorbic acid adsorption.

Table 7
Thermodynamic parameters of ascorbic acid adsorption

Adsorbent	K-Eucal-20			K-Eucal-40		
R^2	1.000			0.948		
$-\Delta H^\circ$ (kJ/mol)	17.248			86.649		
ΔS° (kJ/K·mol)	0.140			0.376		
$-\Delta G^\circ$ (kJ/mol)	298 K	303 K	313 K	298 K	303 K	313 K
	24.52	25.22	26.62	24.96	27.77	30.75
K_d (L/g)	2.02	2.27	2.82	2.41	6.24	13.80
K_d (dimensionless)	19,758.47	22,174.02	27,577.42	23,553.31	60,974.63	134,843.95
E_a (kJ/mol)	15.62			82.80		
Sticking probability (S^*)	2.02×10^{-4}			2.56×10^{-16}		

ascorbic acid adsorption onto K-Eucal-20 and K-Eucal-40 samples at different temperatures is spontaneous. Also, the negative values of ΔH° and their magnitude are both an indication that adsorption processes were taken place via physisorption (for the case of K-Eucal-20) and chemisorption (for the case of K-Eucal-40) associated with exothermicity in both cases.

KOH activation is mostly a chemical to create a more porous surface. In the case of more concentrated KOH (K-Eucal-40) probably we are creating more functional groups that are causing stronger binding which is in accordance with chemisorption process. One can conclude that chemical functionalization is happening in the case of high concentration KOH.

Increasing the temperature from 298 to 313 K, promotes the diffusion of molecules across the outer boundary layer and the internal pores of the adsorbent which has a negative effect on the ascorbic acid adsorption rate.

The positive values of ΔS° indicate the increased randomness at the adsorbent–adsorbate interface during the adsorption process and a good affinity of ascorbic acid towards K-Eucal-20 and K-Eucal-40 adsorbents.

Two other parameters of great utility, the activation energy (E_a) and sticking probability (S^*) estimated from the experimental data are commonly to support the adsorption mechanism predominance [37]. The relationships between the above-mentioned parameters and the surface coverage:

$\theta = (1 - C_e/C_i)$ are given by the modified Arrhenius-type equations in its linearized form [Eq. (13)]. E_a and S^* values are obtained from the slope and the intercept of $\ln(1-\theta)$ vs. $(1/T)$ plots represented by (Fig. 10b) and is summarized in Table 7.

Comparable with ΔH° , the positive values of E_a and their magnitudes confirm the physisorption of ascorbic acid onto K-Eucal-20 and its chemisorption onto K-Eucal-40 associated with exothermicity in both cases. Defined as a measure of the potential of a sorbate to remain on the sorbent indefinitely which is in relation the proportion of collisions with its surface leading to adsorption and depending on the system temperature. S^* values were estimated from the surface coverage (θ) in the temperature range of 298–313 K as shown in Table 7. The obtained results suggest that the probability of ascorbic acid to stick very well on both adsorbents surfaces since $0 < S^* < 1$, confirming that the adsorption processes are favourable (physisorption mechanism is dominant for the case of K-Eucal-20) and (chemisorption mechanism is dominant for the case of K-Eucal-40) according to the following classification: $S^* > 1$ (Sorbate unsticking to sorbent: weak adsorption exist), $S^* = 1$ (linear sorbate–sorbent relation of sticking exists: existence of both chemisorption and physisorption mechanisms), $S^* = 0$ (Indefinite sticking of sorbate to sorbent: chemisorption mechanism is dominant) and $0 < S^* < 1$ (Favourable sticking of sorbate to sorbent: physisorption mechanism is dominant).

4. Conclusion

Treatment of pharmaceutical-laden wastewater using activated carbon derived from raw and carbonaceous *Eucalyptus camaldulensis* leaves was the aim of this investigation. A two-step route using impregnation of ground leaves into potassium hydroxide solutions at different concentration followed by pyrolysis at 600°C for 2 h was performed to enhance uptake rate. Different characterization methods were performed on obtained sample. Significant improvements in surface area (from 92 to 200 m²/g) and uptake (190.80–305.78 mg/g) were noticed. A quick equilibrium time was reached for batch adsorption experiments at ambient temperature. Ascorbic acid adsorption was best described by Langmuir model at working conditions (contact time = 30 min, carbon dosage = 4 g/L and pH = 2.5). Adsorption process was taken place via physisorption associated with and spontaneity at different temperatures. Kinetics was found to obey the pseudo-second-order model and thermodynamic analysis confirms the spontaneity and endothermicity of ascorbic acid adsorption process. This study shows that activated *Eucalyptus camaldulensis* leaves can be successfully used as an alternative to the commercially available adsorbents for the removal of such pollutant from pharmaceutical wastewater industries.

Declaration of interests

The authors declare that they have no known competing financial interests or personal relationships that could have appeared to influence the work reported in this paper.

Acknowledgment

Authors thank the financial support from National PRFU project (Mostaganem University) Code: A16N01UN270120220002 01/01/2022 of the Ministry of Higher Education, Algeria.

And the Department of Catalytic and Sorbent Materials Engineering, Faculty of Chemical Technology and Engineering-West Pomeranian University of Technology in Szczecin (Poland) for providing samples characterization.

References

- [1] F. Thomas, Felicity & World Health Organization, Regional Office for Europe, Pharmaceutical Waste In The Environment: A Cultural Perspective, Public Health Panorama, 2017, pp. 127–132. Available at: <https://apps.who.int/iris/handle/10665/254734>.
- [2] R. John White, A. Marco Belmont, D. Chris Metcalfe, Pharmaceutical compounds in wastewater: wetland treatment as a potential solution, *Sci. World J.*, 6 (2006) 1731–1736.
- [3] M. Patel, R. Kumar, K. Kishor, T. Mlsna, C.U. Pittman Jr., D. Mohan, Pharmaceuticals of emerging concern in aquatic systems: chemistry, occurrence, effects, and removal methods, *Chem. Rev.*, 119 (2019) 3510–3673.
- [4] F.R. Spellman, Handbook of Water and Wastewater Treatment Plant Operations, CRC Press, FL, Boca Raton, 2013.
- [5] M. Zupanc, T. Kosjek, M. Petkovšek, M. Dular, B. Kompare, B. Širok, Ž. Blažeka, E. Heath, Removal of pharmaceuticals from wastewater by biological processes, hydrodynamic cavitation and UV treatment, *Ultrason. Sonochem.*, 20 (2013) 1104–1112.
- [6] A.F. Almomani, M. Shawaqfah, R.R. Bhosale, A. Kumar, Removal of emerging pharmaceuticals from wastewater by ozone-based advanced oxidation processes, *Environ. Prog. Sustainable Energy*, 35 (2016) 982–995.
- [7] B.K. Zaied, M. Rashid, M. Nasrullah, A.W. Zularisam, D. Pant, L.A. Singh, A comprehensive review on contaminants removal from pharmaceutical wastewater by electrocoagulation process, *Sci. Total Environ.*, 726 (2020) 138095, doi: 10.1016/j.scitotenv.2020.138095.
- [8] M.N. Rashed, Adsorption Technique for the Removal of Organic Pollutants from Water and Wastewater, M. Nageeb Rashed, Ed., Organic Pollutants – Monitoring, Risk and Treatment, InTechOpen, 2013, pp. 168–194.
- [9] J. Akhtar, N.A.S. Amin, K. Shahzad, A review on removal of pharmaceuticals from water by adsorption, *Desal. Water Treat.*, 57 (2016) 12842–12860.
- [10] S. Karunya, S. Feroz, S. Al Harassi, K. Sakhile, Treatment of Oman pharmaceutical industry wastewater using low-cost adsorbents, *J. Multidiscip. Eng. Sci. Technol (JMEST)*, 2 (2015) 339–341.
- [11] A. Macias-García, J. García-Sanz-Calcedo, J.P. Carrasco-Amador, R. Segura-Cruz, Adsorption of paracetamol in hospital wastewater through activated carbon filters, *Sustainability*, 11 (2019) 2672, doi: 10.3390/su11092672.
- [12] M. Finn, G. Giampietro, D. Mazyck, R. Rodriguez, Activated carbon for pharmaceutical removal at point-of-entry, *Processes*, 9 (2021) 1091, doi: 10.3390/pr9071091.
- [13] G. Oliveira, V. Calisto, S.M. Santos, M. Otero, V.I. Esteves, Paper pulp-based adsorbents for the removal of pharmaceuticals from wastewater: a novel approach towards diversification, *Sci. Total Environ.*, 631–632 (2018) 1018–1028.
- [14] Ç. Sarıçı-Özdemir, Y. Önal, Statistical analysis of equilibrium and kinetic data for ascorbic acid removal from aqueous solution by activated carbon, *Desal. Water Treat.*, 51 (2013) 4658–4665.
- [15] R. Júlia de Andrade, M.F. Oliveira, M.G.C. da Silva, M.G.A. Vieira, Adsorption of pharmaceuticals from water and wastewater using nonconventional low-cost materials: a review, *Ind. Eng. Chem. Res.*, 57 (2018) 3103–3127.
- [16] J. Yasin, R. Pravinkumar, Production of activated carbon from bio-waste materials by chemical activation method, *AIP Conf. Proc.*, 2225 (2020) 070005, doi: 10.1063/5.0005666.
- [17] ASTM, Standard Test Method for Determination of Iodine Number of Activated Carbon, ASTM Annual Book, 4 (1999) D4607–94, Section 15.
- [18] O. Douinat, B. Bestani, N. Benderdouche, A. Boucherdoud, Use of *Olea europaea* leaves-based activated carbon for pollutant removal from liquid effluents, *Desal. Water Treat.*, 210 (2021) 258–272.
- [19] Z. Mekibes, B. Bestani, N. Douara, N. Benderdouche, M. Benzekri-Benallou, Simultaneous activation of *Ficus carica* L. leaves for the removal of emerging pollutants from aqueous solutions, *Desal. Water Treat.*, 222 (2021) 322–335.
- [20] Á. Simay, L. Gy. Nagy, L. Noszkó, A. Bóta, Preparation of activated carbon from the by-products of agricultural industry, *Period. Polytech., Chem. Eng.*, 28 (1984) 293–297.
- [21] C.-F. Chang, C.-Y. Chang, W.-T. Tsai, Effects of burn-off and activation temperature on preparation of activated carbon from corn cob agrowaste by CO₂ and steam, *J. Colloid Interface Sci.*, 232 (2000) 45–49.
- [22] M. Kwiatkowski, T. Kopac, An analysis of burn-off impact on the structure microporous of activated carbons formation, *J. Phys. Conf. Ser.*, 936 (2017) 012090, doi: 10.1088/1742-6596/936/1/012090.
- [23] L. Zhou, M. Li, Y. Sun, Y. Zhou, Effect of moisture in microporous activated carbon on the adsorption of methane, *Carbon*, 39 (2001) 773–776.
- [24] Q.Q. Shi, J. Zhang, C.L. Zhang, C. Li, B. Zhang, W.W. Hu, J.T. Xu, R. Zhao, Preparation of activated carbon from cattail and its application for dyes removal, *J. Environ. Sci. (China)*, 22 (2010) 91–97.
- [25] K.S.W. Sing, D.H. Everett, R.A.W. Haul, L. Moscou, R.A. Pierotti, J. Rouquerol, T. Siemieniowska, Reporting physisorption data

- for gas/solid systems with special reference to the determination of surface area and porosity (Recommendations 1984), *Pure Appl. Chem.*, 57 (1985) 603–619.
- [26] M.A. Hubbe, A. Azizian, S. Douven, Implications of apparent pseudo-second-order adsorption kinetics onto cellulosic materials: a review, *BioResources*, 14 (2019) 7582–7626.
- [27] Y.S. Ho, G. McKay, Kinetic models for the sorption of dye from aqueous solution by wood, *Process Saf. Environ. Prot.*, 76 (1998) 183–191.
- [28] W.J. Weber Jr., J.C. Morris, Kinetics of adsorption on carbon from solution, *J. Sanit. Eng. Div.*, 89 (1963) 31–60.
- [29] A. Zerhouni, B. Bestani, S. Attouti, N. Benderdouche, Capture Of toxic pollutants by *Pistacia lentiscus* leaves as a low-cost biosorbent: equilibrium, kinetics and thermodynamic studies, *Indian J. Environ. Prot.*, 41 (2021) 723–735.
- [30] H.M.F. Freundlich, Over the adsorption in solution, *J. Phys. Chem.*, 57 (1906) 385–470.
- [31] I. Langmuir, The constitution and fundamental properties of solids and liquids. Part I. Solids, *J. Am. Chem. Soc.*, 38 (1916) 2221–2295.
- [32] M.I. Temkin, V. Pyzhev, Kinetics of ammonia synthesis on promoted iron catalysts, *Acta Phys. U.R.S.S.*, 12 (1940) 217–222.
- [33] K. Sedigheh, M. Asadi, G. Absalan, Adsorption of folic acid, riboflavin, and ascorbic acid from aqueous samples by Fe₃O₄ magnetic nanoparticles using ionic liquid as modifier, *Anal. Methods*, 6 (2014) 798–806.
- [34] R. Ansari, N. Alizadeh, S.M. Shademan, Application of silica gel/polyaniline composite for adsorption of ascorbic acid from aqueous solutions, *Iran. Polym. J.*, 22 (2013) 739–748.
- [35] S.A. Abdel-Gawad, H.M. Abd El-Aziz, Removal of pharmaceuticals from aqueous medium using entrapped activated carbon in alginate, *Air Soil Water Res.*, 12 (2019) 1–7.
- [36] H. Marbawi, A.R. Othman, M.I.E. Halmi, J.A. Gansau, K. Sabullah, N.A. Yasid, Re-evaluation of thermodynamic parameters using dimensionless Langmuir constants from published data on glyphosate adsorption onto activated carbon loaded with manganese and iron, *J. Environ. Biorem. Toxicol.*, 3 (2020) 6–10.
- [37] D.Z. Marković-Nikolić, M.D. Cakić, G. Petković, G.S. Nikolić, Kinetics, thermodynamics and mechanisms of phosphate sorption onto bottle gourd biomass modified by (3-chloro-2-hydroxypropyl) trimethylammonium chloride, *Prog. React. Kinet. Mech.*, 44 (2019) 267–285.